DOI: 10.1002/ejic.200901093

Nanostructured Dioxomolybdenum(VI) Catalyst for the Liquid-Phase Epoxidation of Olefins

Alichandra Castro,[a] João C. Alonso,[b] Anabela A. Valente,*[a] Patrícia Neves,[a]
Paula Brandão,[a] Vitor Félix,[a] and Paula Ferreira*[b]

Keywords: Molybdenum / Mesoporous materials / Heterogeneous catalysis / Epoxidation

A new organosilica hybrid mesoporous material (HM) containing phosphane oxide surface groups was prepared via the "dual" organosilane templated co-condensation of 4-bis(triethoxysilyl)benzene and (diphenylphosphanyl)propyltriethoxysilane, followed by post-synthesis oxidation of the phosphane surface groups. The HM material was used to immobilise the [$Mo(O)_2Cl_2$] complex. The resultant material (HM-Mo) is an active and selective catalyst in the liquid-phase epoxidation of olefins [*cis*-cyclooctene, (*R*)-(+)-limonene, *trans*-2-octene, 1-octene] with *t*BuOOH at 55 °C and gives comparable epoxide yields to those observed for the free complex [$MoCl_2(O)_2\{OP(CH_2CH_3)(Ph)_2\}_2$] (**1**), under similar reaction conditions: the crystal structure of complex **1** remains the same after reaction with *t*BuOOH. The oxidant is essentially consumed in the HM-Mo or **1** catalysed epoxidation of the olefin. In the case of limonene (possesses endo- and exocyclic C=C bonds), the molar ratio of 1,2-epoxy-*p*-menth-8-ene/1,2–8,9-diepoxy-*p*-menthane at ca. 90 % conversion (reached after 24 h reaction) is ca. 5 and 10 for **1** and HM-Mo, respectively, indicating a favourable regioselectivity towards the epoxidation of the endocyclic C1–C2 double bond, especially in the case of the heterogeneous catalyst.

Introduction

Organic–inorganic hybrid materials are particularly attractive for preparing a wide range of multifunctional materials with potential commercial applications. They are prepared by the combination of organic and inorganic components, allowing a synergy of the thermal stability and chemistry of ceramic materials with the relatively easy processability and flexibility of organic compounds and polymers.[1] In recent years, ordered mesoporous silicon-containing hybrid materials (MesoSiHyb) prepared via co-condensation of organosilanes in the presence of a template have become attractive catalyst supports partly due to their good mechanical strength, thermal and chemical stability (e.g., in oxidation environment), versatility (the physicochemical properties can be modified/fine-tuned through changes in compositions, architectures and functionalities during the process of material synthesis), high specific surface area and large pore sizes.[2]

The metal-catalysed epoxidation of olefins into epoxides is an important reaction in organic synthesis, as epoxides are useful intermediates that can be transformed into a variety of other compounds.[3–6] Molybdenum complexes are used as catalysts in industrial liquid-phase epoxidation processes.[6] Molybdenum(VI) complexes of the type [$MoO(O_2)_2(OPR_3)(H_2O)$] (R = alkyl ligands) are of commercial interest as homogeneous epoxidation catalysts (patented by BASF[7]): complexes of this type were first introduced as epoxidation catalysts with hexamethylphosphoramide instead of (OPR_3) in pioneering studies carried out by the group of Mimoun.[8]

Molybdenum(VI) complexes of the type [$Mo(O)_2Cl_2$] and related complexes bearing organic ligands have been used as catalysts for various organic transformations,[9] including the selective epoxidation of olefins with *tert*-butyl hydroperoxide (*t*BuOOH).[10–18] However, these metal complexes are homogeneous catalysts, and it is desirable to heterogenise them, because important advantages of heterogeneous catalysts are the easier product–catalyst separation and catalyst reuse. For liquid-phase heterogeneous catalytic processes, the catalyst stability towards solvation/leaching of active species is one of the major concerns. Complexes of the type [$Mo(O)_2Cl_2L$], where L = O- or N-containing ligand(s), have been covalently anchored onto micelle-templated ordered mesoporous silicas (e.g., MCM-41, MCM-48, SBA-15) via one of the following routes: (i) by directly adding the prepared metal complex to the silica support or (ii) pretreating the silica with L and subsequent introduction of the metal precursor (so-called tethering approach).[19–22] Although this group of catalysts is quite effective in the epoxidation of olefins with *t*BuOOH, it presents at least some of the following disadvantages: (i) heterogeneous distribution of active species, (ii) different active

---

[a] Department of Chemistry, CICECO, University of Aveiro,
3810-193 Aveiro, Portugal
E-mail: atav@ua.pt
[b] Department of Ceramics and Glass Engineering, CICECO,
University of Aveiro,
3810-193 Aveiro, Portugal
Fax: +351-234401470
E-mail: pcferreira@ua.pt

sites formed via the reaction of the molybdenum precursor with the (un)functionalised silica support (e.g., the metal precursor may react with silanol or L surface groups), (iii) partial metal leaching during catalysis. Improvements concerning the stability towards metal leaching and catalytic activity have been accomplished through treating the mesoporous silica surface with $(CH_3)_3SiCl$, which enhances the surface hydrophobicity.[21,23,24] Fairly good catalyst stability has been reported for polystyrene resin functionalised with phosphane groups, and they have been subsequently grafted with $[Mo(CO)_6]$ and used in the catalytic epoxidation of aromatic and aliphatic terminal alkenes with *t*BuOOH [most likely the supported metal species are oxidised to molybdenum(VI)].[25] Alternatively, efficient solid epoxidation catalysts have been prepared by supporting molybdenum(VI) complexes on MesoSiHyb materials via ligand exchange reactions.[26,27]

Recently, some of us reported on the catalytic performance of a mesostructured hybrid materials prepared by introducing $[Mo(O)_2Cl_2]$ in a preformed mesoporous silica functionalised with phosphane oxide spacer ligands:[28] in general, epoxide selectivity was excellent, albeit the occurrence of Mo and P leaching during catalysis and a concomitant decrease in catalytic activity of the used catalyst was observed, which could be related to the diversity of surface metal species. In this work, a new hybrid mesoporous material (HM) has been prepared by co-condensation of the organosilanes 1,4-bis(triethoxysilyl)benzene (BTEB – carries the organic component of the matrix) and (diphenylphosphanyl)propyltriethoxysilane (TEPPP – for pending phosphane groups) in the presence of Pluronics P123 as a template, followed by template removal (through chemical treatment) and post-synthesis oxidation of the phosphane surface groups into phosphane oxide. The resultant HM material is used as a support for grafting $[Mo(O)_2Cl_2]$, giving a new catalyst (HM-Mo) for the liquid-phase epoxidation reaction of olefins with *t*BuOOH. The investigated olefins are *cis*-cyclooctene, (*R*)-(+)-limonene, *trans*-2-octene and 1-octene, and the catalytic reactions were carried out at 55 °C, without a cosolvent. For comparative studies the complex $[MoCl_2(O)_2\{OP(CH_2CH_3)(Ph)_2\}_2]$ (**1**) was prepared and tested as a catalyst, under similar conditions. The crystal structure of complex **1** is also reported.

Results and Discussion

Preparation and Characterisation of the Catalysts

Complex 1

The complex $[MoCl_2(O)_2\{OP(CH_2CH_3)(Ph)_2\}_2]$ (**1**) is obtained by treating $[Mo(O)_2Cl_2]$ with two equivalents of the phosphane oxide ligand $CH_3CH_2(Ph)_2PO$. The molecular structure of **1** excluding the hydrogen atoms (Figure 1) has a distorted octahedral coordination sphere with equatorial coordination of the molybdenum centre composed of four oxygen atoms from two O=Mo groups (oxo) and two diphenylphosphane oxide ligands (dppeO). The bond lengths and angles subtended at the molybdenum centre compare well with those found for the related complex $[Mo(O)_2Cl_2(OPMePh_2)_2]$.[29]

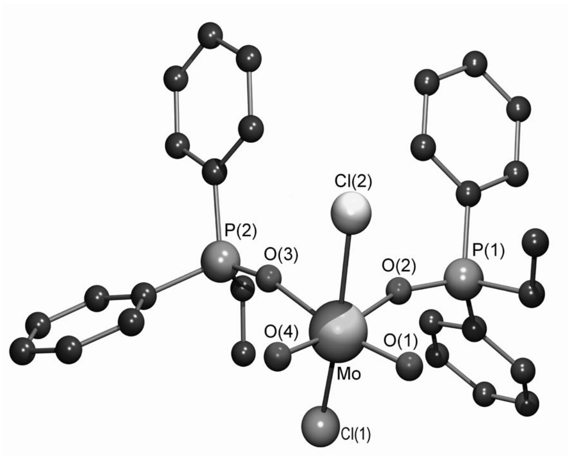

Figure 1. Molecular diagram showing the overall geometry of complex $[MoCl_2(O)_2\{OP(CH_2CH_3)(Ph)_2\}_2]$ (**1**) with labelling scheme adopted.

Mesostructured Material HM-Mo

The co-condensation of BTEB and TEPPP in the presence of a template, followed by the removal of the latter and, finally, the oxidation of the surface phosphane surface groups into phosphane oxide (complete as monitored by ^{31}P CP MAS NMR), gives HM (Scheme 1). The complex $[Mo(O)_2Cl_2]$ was grafted onto HM to give HM-Mo with 0.47 mmol g^{-1} of Mo and a P/Mo mol ratio of 1.8.

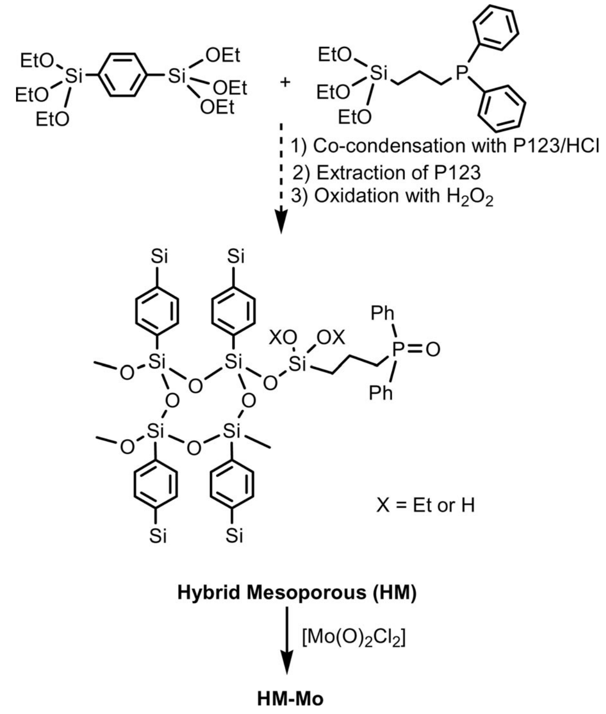

Scheme 1. Schematic synthesis of heterogeneous catalyst.

The powder XRD patterns of both HM and HM-Mo evidence diffraction at 2*θ* at ca. 0.91°, indicating some mesoporous order, which is supported by TEM showing a hexagonal arrangement of mesoporous (Figure 2 for HM-Mo). The typical short range order usually observed when phenylene groups are present in the material[30] was not observed, suggesting that the molecular scale periodicity is perturbed by the introduction of the bulky phosphane oxide ligands. This may also explain the unclear presence of the (110), (200), (210) and (300) reflections. Another explanation for the lack of molecular scale periodicity is the synthesis under acidic conditions, which is not favourable for the formation of a periodic arrangement of the phenylene-silica moieties as reported by Inagaki and co-workers.[31]

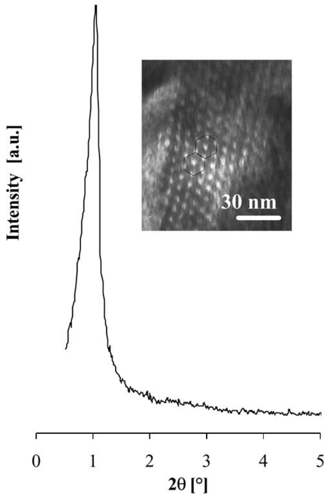

Figure 2. Powder X-ray diffraction pattern and TEM image (inset) of HM-Mo.

The HM and HM-Mo materials exhibit irreversible type IV nitrogen adsorption–desorption isotherms (characteristic of mesoporous solids) with relatively sharp capillary condensation steps in the relative pressure range 0.5–0.62 (Figure 3).[32] The nitrogen uptake of HM-Mo is slightly lower than that of HM, leading to a concomitant reduction in BET specific surface area and total pore volume (Table 1). The pore-size distribution (PSD) curves are relatively narrow with a maximum d_p of 6.1 and 5.8 nm for HM and HM-Mo, respectively. The pore-wall thickness calculated as $[(2d_{100}/\sqrt{3}) - d_p]$, where the first term represents the lattice parameter considering a hexagonal unit cell, is 5.1 nm for HM. These results, together with the powder XRD and TEM data, indicate that the (fairly ordered) mesoporous structure of HM is preserved during the post-synthesis grafting procedure and suggest that the metal complex is grafted on the internal surface of HM.

The ^{29}Si CP MAS NMR spectra of HM and HM-Mo display three signals at δ = –69.9, –77.0 and –80.0 ppm, assigned to T^1, T^2 and T^3 organosilica species [$T^m = \mathrm{R}Si(\mathrm{OSi})_m(\mathrm{OH})_{3-m}$], respectively (Figure 4). No Q^n species were identified in the spectra, indicating that silanol surface groups are negligible (or inexistent) and that the Si–C bond is preserved (e.g., resistant to hydrolysis) during the (post-)synthesis processes.

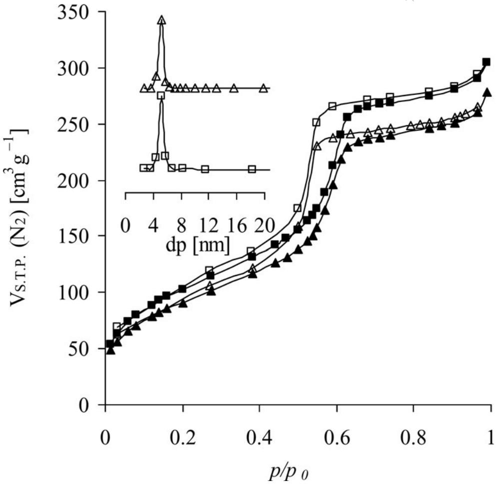

Figure 3. Nitrogen adsorption–desorption isotherms and pore-size distribution curve of HM (open square) and HM-Mo (open triangle).

Table 1. Texture parameters of the hybrid materials.

Sample	S_{BET} [a] [m^2 g^{-1}]	V_P[b] [cm^3 g^{-1}]	d_p[c] [nm]
HM	437	0.51	6.1
HM-Mo	335	0.43	5.8

[a] BET specific surface area, relative pressure range 0.03–0.15. [b] Specific total pore volume by using the Gurvitsch equation for relative pressure of ca. 0.98. [c] Maximum of the pore-size distributions calculated by the BJH method by using the nitrogen adsorption data.

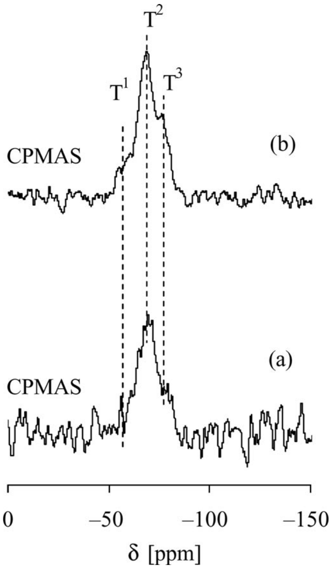

Figure 4. ^{29}Si CP MAS NMR spectra of the HM materials: (a) HM and (b) HM-Mo.

The ^{13}C CP MAS NMR spectrum of HM-Mo shows resonances at δ = 15.6 (CH_3) and 57.8 ppm (CH_2) due to (reminiscent) [SiO–CH_2CH_3] groups (Figure 5). The resonances at δ = 62.5 and 30.0 ppm are assigned to the first and second (counting from the left) methylene groups in [P$CH_2CH_2CH_2$Si], respectively. One could expect the signal related with the methylene group bonded to the silicon atom in [P$CH_2CH_2CH_2$Si] to appear at higher field, which is probably overlapped with that of the methyl group in [SiO–CH_2CH_3]. The peak at δ = 73 ppm is assignable to the residual template.

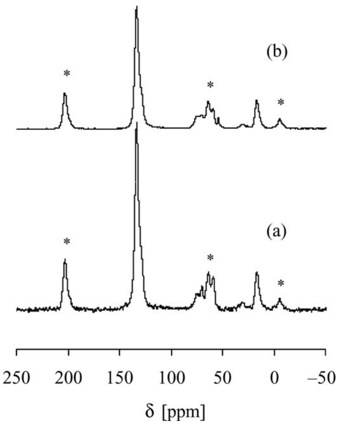

Figure 5. ^{13}C CP MAS NMR spectra of the HM materials: (a) HM and (b) HM-Mo. The symbol * denotes spinning sidebands.

The ^{31}P CP MAS spectra of HM and HM-Mo show a peak at δ = 36.9 ppm, assigned to P^V species (Figure 6). A small shoulder at ca. δ = 21.0 ppm can be observed in both spectra and may be attributed to a side reaction during the synthesis procedure to give P^V species of the type $(EtO)_3$-$Si(CH_2)_3(Ph)_2P(\text{-O-}[SiO_2])_2$ (this phosphorus atom is not available to coordinate the molybdenum).[33]

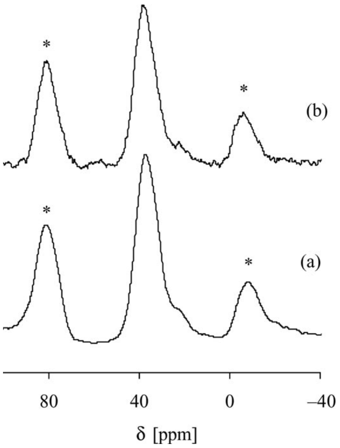

Figure 6. ^{31}P CP MAS NMR spectra of the HM materials: (a) HM and (b) HM-Mo. The * symbol denotes spinning sidebands.

Catalysis Studies

The catalytic performance of HM-Mo was investigated in the epoxidation of *cis*-cyclooctene (Cy8) with *t*BuOOH at 55 °C without a cosolvent. For comparative purposes, the reaction was carried out in the presence of complex **1**, under similar reaction conditions. A control experiment was performed by using $OP(Ph)_2CH_2CH_3$ (completely soluble in the reaction medium) instead of complex **1**, which gives cyclooctene oxide and cyclooctane-1,2-diol as the only products formed in 73 and 27% selectivity, respectively, at 10% conversion (reached after 24 h; Figure 7). Another control experiment consisted of performing the reaction of Cy8 in the presence of HM (without Mo), which is very sluggish, giving 7% conversion after 24 h: the main product was cyclooctene oxide (75% selectivity) and cyclooctane-1,2-diol was the byproduct (Figure 7). Iodometric titrations were performed for the reaction of *t*BuOOH in the presence of **1** or HM-Mo (without olefin), which indicated that the "nonproductive" decomposition of *t*BuOOH is negligible.

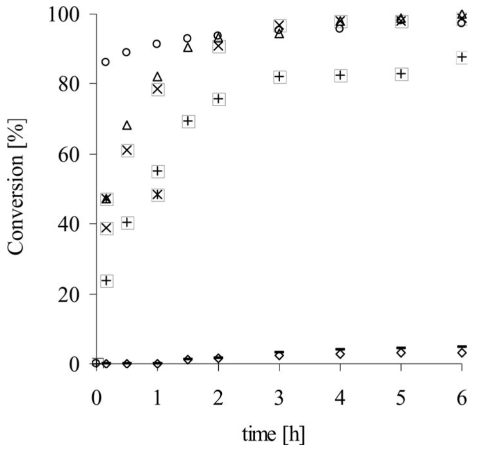

Figure 7. Reaction of *cis*-cyclooctene with *t*BuOOH at 55 °C in the presence of complex **1** [run 1 (○); run 2, (+)], $OP(Ph)_2CH_2CH_3$ (◇), HM-Mo [run 1 (△); run 2 (×)] or HM (–); leaching test performed for HM-Mo (catalyst filtration at 10 min; *).

Catalytic Performance of Complex 1

The reaction of Cy8 with *t*BuOOH in the presence of complex **1** gives quantitative epoxide yield after 24 h (Table 2). The catalytic activity of **1** is comparable to that reported in the literature for $[MoCl_2(O)_2\{OP(Ph)_2CH_3\}_2]$, used as a catalyst in the same reaction, under similar conditions: TOF calculated for a 30 min reaction is 150 and 179 $\text{mol}\,\text{mol}_{Mo}^{-1}\,h^{-1}$ for $[MoCl_2(O)_2\{OP(Ph)_2CH_3\}_2]$ and **1**, respectively.[34] Relatively high catalytic activity in olefin epoxidation with *t*BuOOH was also reported in the case of the complex $[Mo(O)_2C1_2L]$, where L is a 3-(diethoxyphosphoryl) derivative of camphor.[35]

In the case of complex **1**, after 10 min, 86% conversion was reached, and afterwards the reaction slowed down considerably (Figure 7). During the course of the catalytic reaction *tert*-butyl alcohol (*t*BuOH), a byproduct associated to the consumption of *t*BuOOH, may act as an inhibitor for the coordination of the oxidant to the metal centre.[36–41] On the basis of the mechanistic considerations reported in the literature for complexes possessing the $[Mo(O)_2]^{2+}$ moiety and Lewis base N,O,S ligands, used as catalysts in the same reaction, the oxidant coordinates to the metal centre to give an (electrophilic) active oxidising specie responsible for the oxygen atom transfer to the (nucleophilic) olefin.[42–45] Electrophilic attack of the oxidant on the C=C bond has also been reported for complexes of the type

Table 2. Reaction of olefins with *t*BuOOH in the presence of different catalysts over 4/24 h at 55 °C.[a]

Olefin	Catalyst	Conv.[b] [%]	Sel.[c] [%]	Yield[d] [%]
cis-Cyclooctene	**1**	97/100	100/100	97/100
	HM-Mo	98/100	100/100	98/100
	HM	4/7	100/75	4/5
	none	1/4	100/100	1/4
(*R*)-(+)-Limonene	**1**	86/93	84/79[e]	72/73
	HM-Mo	80/91	85/86[e]	68/78
1-Octene	**1**	28/48	100/100	28/48
	HM-Mo	24/45	100/100	24/45
trans-2-Octene	**1**	57/79	100/100	57/79
	HM-Mo	59/80	100/100	59/80

[a] Reaction conditions: olefin (1.8 mmol), *t*BuOOH (2.75 mmol), complex **1** (18 µmol) or HM-Mo (17.3 mg, 8.1 µmol Mo). [b] Olefin conversion after 4/24 h. [c] Selectivity to the corresponding epoxide (limonene oxide in the case of limonene) after 4/24 h. [d] Epoxide yield after 4/24 h. [e] Selectivity to 1,2–8,9-diepoxy-*p*-menthane after 4/24 h is 9/16% and 7/8% for **1** and HM-Mo, respectively.

[$MoO(O_2)_2(OPR_3)$] (R = alkyl), albeit involving different transition states.[46,47]

After the first 24-h run, a second run was carried out by recharging the reaction vessel with oxidant and substrate (in the same amounts as those used in the first run), and by monitoring the catalytic reaction for a further 24 h. Quantitative epoxide yield was obtained in two consecutive 24-h runs, albeit the reaction was slower in the second run (at least until 6 h), which may be due to dilution effects and/or the presence of *t*BuOH at the beginning of the second run. These two factors may be avoided by using a heterogeneous catalyst and by separating it from the reaction products prior to its reuse (see next section).

A separate (larger scale) experiment was performed by mixing complex **1** with *t*BuOOH (1:20 molar ratio) without olefin for 3 h at 55 °C. After cooling to room temperature, *n*-hexane was added until a precipitate was obtained, which was separated by centrifugation, washed with *n*-hexane and dried at room temperature. Subsequently, the solid was dissolved in dichloromethane, and this solution was left under static conditions for approximately one month to give crystals that were separated by filtration, washed with *n*-hexane and dried at room temperature (the resultant compound is denoted **1**rec_crystal). Single-crystal XRD showed that the structure of **1**rec_crystal is similar to that of complex **1**: these results were reproducible for different crystals in the sample. The FTIR spectrum of **1**rec_crystal is very similar to that of **1** (Figure 8). Hence, complex **1** is stable, at least to a certain extent, under the applied oxidising conditions.

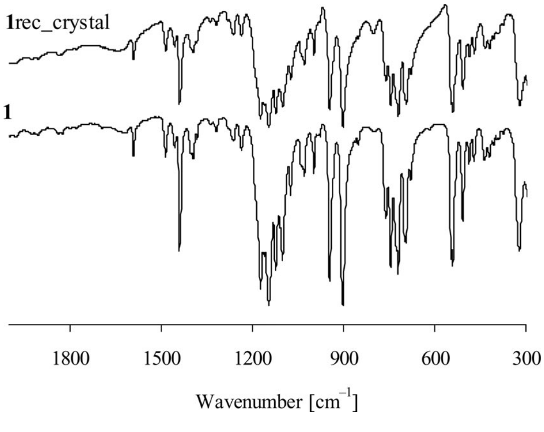

Figure 8. FTIR spectra of **1** and **1**rec_crystal (compound recovered after treatment under catalytic conditions).

Catalytic Performance of HM-Mo

The HM-Mo catalyst gives quantitative epoxide yield within 6 h (Figure 7). Similar results (100% epoxide yield at 4 h) were recently reported for complexes of the type [$MoO(O_2)_2L$] {L = (3-triethoxysilylpropyl)-[3-(2-pyridyl)pyrazol-1-yl]acetamide} supported on phenylene-bridged mesoporous organosilicas, used as catalyst in the same reaction, and chloroform (b.p. 61.2 °C) as solvent, under reflux.[48] Initial TOF (calculated for 10 min reaction) is 541 $mol\,mol_{Mo}^{-1}\,h^{-1}$ for HM-Mo, which is comparable with that observed for complex **1** (519 $mol\,mol_{Mo}^{-1}\,h^{-1}$), suggesting that the nature of the active species involved may be similar. The lower conversions reached at the beginning of the reaction in the presence of HM-Mo in relation to that observed for complex **1** may be, at least partly, due to the lower amount of molybdenum species loaded into the reaction vessel in the former case (similar conversions are reached after 90–120 min).

To assess the homo/heterogeneous nature of the catalytic reaction in the presence of HM-Mo a leaching test was performed by filtering off (at 55 °C) the reaction solution after 10 min, through a 0.2 µm PVDF w/GMF Whatman membrane, and leaving it to react for a further 50 min at 55 °C. No increase in olefin conversion was observed after the filtration step, whereas in the presence of HM-Mo conversion increased by ca. 35%. These results suggest that the olefin epoxidation reaction with HM-Mo as catalyst is heterogeneous in nature. The FTIR spectra of the fresh and recovered solids were identical (not shown). The recovered HM-Mo catalyst (washed with *n*-hexane and dried at room temperature) was reused in a second 24 h run at 55 °C. After reaction, the solid catalyst was separated by centrifugation, thoroughly washed with *n*-hexane and dried at room temperature overnight. Epoxide selectivity was always 100%. The kinetic curves for the two 24-h runs are roughly coincident (Figure 7), and ICP-AES analyses of the recovered solid indicated no measurable Mo or P leaching. High catalyst stability has also been reported by the group of Thiel for (i) complexes of the type [$MoO(O_2)_2$] supported on hybrid supports synthesised by sol–gel copolymerisation of a chelate ligand with TEOS,[26,27] and (ii) the complex [$MoO(O_2)_2L$] {L = (3-triethoxysilylpropyl)-[3-(2-pyridyl)pyrazol-1-yl]acetamide} supported on a hydrophobic phenylene-bridged mesoporous organosilica.[48] The catalytic performance of HM-Mo is superior to that recently reported for a catalyst prepared by tethering [$Mo(O)_2Cl_2$] onto a preformed mesoporous silica functionalised with phosphane oxide spacer ligands:[28] Mo and P leaching and a concomitant decrease in catalytic activity were observed for the used catalyst. The higher catalyst stability of HMo in comparison to the catalyst prepared through the tethering synthetic approach may be related to its hydrophobic, uniform, single-site features.

The HM-Mo catalyst was further tested in the reactions of (*R*)-(+)-limonene, 1-octene and *trans*-2-octene with *t*BuOOH at 55 °C without a cosolvent: the same reactions were carried out in the presence of complex **1** for comparison (Table 2). Interestingly the homogeneous and heterogeneous catalysts give similar conversions and epoxide yields at 4/24 h for all the olefins, under the applied reaction conditions. The linear olefins 1-octene and *trans*-2-octene give the respective epoxides as the only products. The epoxides yields at 4 h are 24–28 and 57–59% for 1-octene and *trans*-2-octene, respectively, indicating that the latter is more reactive than the former. The higher reactivity of the more substituted (electron richer) olefin than the less substituted one is congruent with the above mechanistic considerations: as a result of the electrophilic nature of oxygen transfer, more nucleophilic olefins tend to react faster. The reaction of limonene gives mainly 1,2-epoxy-*p*-menth-8-ene (P1) formed in 68–72% yield after 4 h. Byproducts include mainly 1,2-8,9-diepoxy-*p*-menthane (P2), *p*-menta-1,8-dien-7-ol and 4-isopropyl-1-methylcyclohexane-1,2-diol. The molar ratio P1/P2 at ca. 90% conversion (reached at 24 h reaction) is ca. 5 and 10 for **1** and HM-Mo, respectively, indicating a favourable regioselectivity towards the epoxidation of the endocyclic C1–C2 double bond. The significantly higher P1/P2 molar ratio observed for the supported catalyst in comparison to complex **1** may be due to confinement effects.

Conclusions

A nanostructured catalyst (HM-Mo) was prepared by grafting of the molybdenum precursor [$Mo(O)_2Cl_2$] to a novel hybrid mesoporous support containing phosphane oxide surface groups (HM). The HM material is prepared by the "dual" organosilane co-condensation method, followed by template (Pluronics P123) removal and post-synthesis oxidation of the phosphane surface templated groups into phosphane oxide. The two organosilanes are 1,4-bis(triethoxysilyl)benzene, which carries the organic component of the matrix, and (diphenylphosphanyl)propyltriethoxysilane, which accounts for pending phosphane groups.

The HM-Mo material is an active and selective catalyst in the liquid-phase epoxidation of *cis*-cyclooctene (100% epoxide yield at 24 h), (*R*)-(+)-limonene (78% epoxide yield), 1-octene (45% epoxide yield) and *trans*-2-octene (80% epoxide yield) with *t*BuOOH at 55 °C without a cosolvent. Similar results were obtained for complex **1**, under similar reaction conditions. Single-crystal XRD data for complex **1** before and after contact with *t*BuOOH are similar. For complex **1** and HM-Mo, *t*BuOOH is essentially consumed in the epoxidation process. In the case of HM-Mo, no P and Mo leaching was detected and the catalyst could be recovered by simple filtration, washing and drying at room temperature to give similar catalytic results as those observed for the fresh catalyst. The heterogeneous nature of the catalytic reaction was assessed through a leaching test carried out at the reaction temperature. In the case of the limonene reaction, regioselectivity (endo/exo C=C epoxidation, at ca. 90% conversion) to 1,2-epoxy-*p*-menth-8-ene was higher for HM-Mo than for complex **1**, which may be partly due to confinement effects of the nanostructured catalyst.

Overall, it seems that HM-Mo is an interesting, uniform, single-site, mesostructured epoxidation catalyst. It may be interesting to further investigate the effects of the aliphatic chain length and the substituents in the phenyl groups of the phosphane oxide ligand on the catalytic performance and the examination of the reactivity of different substrates. On the other hand, the use of HM and related materials as catalyst supports may be extendable to a plethora of homogeneous catalysts used in different organic reactions (e.g., asymmetric catalysis, hydrogenations). Other promising fields of application include nanomedicine – hundreds of organophosphorus drugs are currently known.

Experimental Section

Materials and Characterisation Techniques: Starting reagents were acquired from Aldrich, and commercial, extra-dried solvents were obtained from Acros Organics ($H_2O < 0.003\%$, AcrosSeal®) and used as received. The catalysts were prepared by using standard Schlenk techniques under a nitrogen atmosphere. Powder X-ray diffraction (PXRD) data were collected with a Philips X′Pert MPD diffractometer (Cu-K_α X-radiation, $\lambda = 1.54060$ Å) fitted with a graphite monochromator and a flat-plate sample holder, in a Bragg–Brentano *para*-focusing optics configuration. Samples were step-scanned in 0.02° 2θ steps with a counting time of 2 s per step; reference material 675 (National Bureau of Standards) was used as internal standard. TEM images were recorded with a 300 eV Hitachi H9000-NA instrument. Nitrogen adsorption isotherms at –196 °C were measured by using a Gemini 2375 Micromeritics Instrument (Eng. M. C. Costa, University of Aveiro). The mesostructured materials were pretreated at 150 °C prior to analysis. Microanalyses for C and H were carried out at the Department of Chemistry, University of Aveiro (M. M. Marques). The P and Mo contents were determined by ICP-AES at the Central Laboratory for Analysis, University of Aveiro (L. Carvalho). Infrared spectra (KBr pellets) were measured by using a Mattson 7000 FT spectrometer. ^{13}C, ^{29}Si and ^{31}P solid-state NMR spectra were recorded at 100.62, 79.49 and 161.98 MHz, respectively, with a (9.4-T) Bruker Avance 400P spectrometer. ^{29}Si MAS NMR spectra were recorded with 40° pulses, spinning rates 5.0–5.5 kHz and 60-s recycle delays. ^{29}Si CP MAS NMR spectra were recorded with 4-μs 1H 90° pulses, 8 ms contact time, a spinning rate of 5 kHz and 4-s recycle delays. For ^{31}P MAS NMR spectra were recorded with 45° pulses, spinning rate of 15 kHz, ^{1}H decoupling and a 60 s recycle delay. Chemical shifts are quoted in parts per million from phosphoric acid (85%). ^{13}C CP MAS NMR spectra were recorded with 4.5-μs 1H 90° pulses, 2 ms contact time, a spinning rate of 7 kHz and 4-s recycle delays. Chemical shifts are quoted in ppm from TMS. ^{13}C spectra were also recorded in the solid state at 125.76 MHz with a Bruker Avance 500 spectrometer.

X-ray Crystallography: Crystals of **1** with suitable quality for single-crystal X-ray diffraction analysis were grown from a dichloromethane solution. The X-ray data were collected with a CCD Bruker APEX II at 150(2) K by using graphite monochromated Mo-K_α radiation (λ = 0.71073 Å). The crystal was positioned at 35 mm from the CCD and the spots were measured by using a counting time of 20 s. Data reduction, including a multiscan absorption correction, were carried out by using the SAINT-NT from Bruker AXS. The structure was solved by using SHELXS-97[49] and refined by using full-matrix least-squares in SHELXL-97.[50] The C–H hydrogen atoms were included at calculated positions, whereas the hydrogen atoms bonded to water molecules were located from final difference Fourier maps. Anisotropic thermal parameters were used for all non-hydrogen atoms, whereas the hydrogen atoms were refined with isotropic parameters equivalent to 1.2 times those of the atom to which they were attached. 19040 reflections were collected and subsequently merged to 6702 unique reflections with a R_{int} of 0.0258. The final refinement of 336 parameters converged to final R and R_{w} indices R_1 = 0.0367 and wR_2 = 0.0933 for 5405 reflections with $I > 2\sigma(I)$ and R_1 = 0.0487 and wR_2 = 0.1002 for all *hkl* data. Molecular diagrams presented are drawn with graphical package software PLATON.[51] Crystal data for **1**: $C_{28}H_{30}Cl_2MoO_4P_2$, M_{r} = 659.33; monoclinic, space group $P2_1/n$, Z = 4, a = 9.4338(2) Å, b = 17.8462(4) Å, c = 17.5228(3) Å, β = 103.3970(10)°, V = 2869.82(10) Å^3, $\rho_{\mathrm{calcd.}}$ = 1.526 Mg m^{-3}, Mo-K_α = 0.787 mm^{-1}. CCDC-744897 contains the supplementary crystallographic data for this paper. These data can be obtained free of charge from the Cambridge Crystallographic Data Centre via www.ccdc.cam.ac.uk/ data_request/cif.

Preparation of the Catalysts

[MoCl$_2$(O)$_2${OP(CH$_2$CH$_3$)(Ph)$_2$}$_2$] (1): Complex **1** was synthesised by following a similar procedure to that described in the literature by Hursthouse et al.[52] Phenylphosphane oxide (0.500 g, 2.17 mmol) was added to a solution of [Mo(O)$_2$Cl$_2$] (0.200 g, 1.00 mmol) in dichloromethane (5 mL) under a nitrogen atmosphere. The solution was stirred for 2 h and then left at 5 °C for 8 d to give a solid containing colourless transparent crystals (0.653 g, yield: 99 wt.-%). The solid was separated by filtration, washed with *n*-hexane and dried at room temperature. $C_{28}H_{30}Cl_2MoO_4P_2$ (659.33): calcd. C 51.01, H 4.59; found C 50.28, H 4.66. ^{1}H NMR (300 MHz, CDCl$_3$, r.t.): δ = 7.30–7.76 (m, 10 H, Ph), 2.45 (9, $^3J_{\mathrm{H,H}}$ = 6.00 Hz, 4 H, PCH_2-), 1.13 (t, $^3J_{\mathrm{H,H}}$ = 6.00 Hz, 6 H, -CH$_2$$CH_3$) ppm. ^{31}P NMR (300 MHz, CDCl$_3$, r.t.): δ = 49 ppm. IR (KBr pellet): $\tilde{\nu}$ = 901, 944 ($\nu_{\mathrm{Mo=O}}$), 1173, 1146 ($\nu_{\mathrm{P=O}}$), 321 ($\nu_{\mathrm{Mo-Cl}}$), 3057 [$\nu_{\mathrm{(C-H)Ph}}$], 1232–1482 [$\nu_{\mathrm{(C-C)Ph}}$], 1238 [$\nu_{\mathrm{p(CH)}}$], 1030 [$\nu_{\mathrm{s(CC)}}$], 719 [$\nu_{\mathrm{op(CH)}}$] cm^{-1}.

Preparation of the Hybrid Mesoporous Material (HM)

Step 1: The 1,4-bis(triethoxysilyl)benzene (BTEB) precursor was prepared by following a procedure previously described.[31]

Step 2: The (diphenylphosphanyl)propyltriethoxysilane precursor (TEPPP) was prepared by a modified procedure of that reported elsewhere:[53] A solution of potassium diphenylphosphide (0.5 M in THF, 20 mL) was added dropwise to a solution of 1-chloro-3-(triethoxysilyl)propane (2.40 mL, 0.01 mol) in THF (20 mL). The mixture was stirred for 3 h at 15 °C and left at room temperature overnight. The work up of the reactions consisted of the evaporation of THF, addition of pentane to precipitate the salt and dissolution of the products. After filtration and evaporation of pentane, the resulting yellow oil was distilled under reduced pressure (1 Torr) at 240 °C. $C_{21}H_{31}O_3PSi$ (390.53): calcd. C 64.59, H 8.00; found C 64.02, H 7.89. ^{1}H NMR (300 MHz, CDCl$_3$, r.t.): δ = 7.20–7.33 (m, 10 H, Ph), 3.79 (q, $^3J_{\mathrm{H,H}}$ = 7.06 Hz, 6 H, OCH_2CH$_3$), 2.06 (t, $^3J_{\mathrm{H,H}}$ = 7.70 Hz, 2 H, PCH_2-), 1.44–1.57 (m, 2 H, CH$_2$$CH_2CH_2$), 1.10 (t, $^3J_{\mathrm{H,H}}$ = 7.06 Hz, 9 H, OCH$_2$$CH_3$), 0.74 (t, $^3J_{\mathrm{H,H}}$ = 7.93 Hz, 2 H, -CH_2Si) ppm. ^{31}P NMR (300 MHz, CDCl$_3$, r.t.): δ = –16.8 ppm. IR (KBr pellet): $\tilde{\nu}$ = 3051 [$\nu_{\mathrm{(C-H)Ph}}$], 1363–1481 [$\nu_{\mathrm{(C-C)Ph}}$], 1294 [$\nu_{\mathrm{p(CH)}}$], 696 [$\nu_{\mathrm{op(CH)}}$], 1074 [ν($_{\mathrm{Si-O}}$)] cm^{-1}.

Step 3: The mesoporous hybrid support was prepared by hydrolysis and co-condensation of BTEB and TEPPP in the presence of Pluronics P123 ($EO_{20}PO_{70}EO_{20}$) as template. In a typical synthesis, the template (0.75 g, 1.32×10^{-4} mol) was dissolved in a mixture of distilled water (29 g, 1.599 mol) and HCl (37 wt.-% aq.; 0.20 mL, 2.25×10^{-3} mol). After addition of the premixed organosilanes, BTEB (0.893 g or 2.22×10^{-3} mol) and TEPPP (0.096 g or 2.46×10^{-4} mol), the reaction mixture was kept at 50 °C for 22 h under vigorous stirring. After hydrothermal treatment for 24 h at 100 °C in a teflon-lined stainless steel autoclave, the obtained precipitate was filtered, washed with distilled water and dried in air overnight. Removal of the template was accomplished by extraction of the as-synthesised solid (0.5 g) with a mixture of 37% HCl (4.5 g) in ethanol (125 mL). The phosphane surface groups were oxidised by using a described literature method[54] to accomplish the HM material.

HM-Supported Mo$^{\mathrm{VI}}$ Catalyst (HM-Mo): The HM material (0.175 g) was impregnated with a solution of [Mo(O)$_2$Cl$_2$] (0.040 g, 2.011×10^{-4} mol) in dichloromethane (5 mL). After stirring the mixture overnight at room temperature, HM-Mo was separated by filtration, washed three times with dichloromethane and dried under vacuum at room temperature.

Catalysis: The liquid-phase olefin epoxidation reactions were carried out in air and autogenous pressure, in batch microreactors equipped with a magnetic stirrer and a sampling valve, and immersed in an oil bath heated at 55 °C. Typically, the reaction vessels were loaded with the olefin (1.8 mmol), *t*BuOOH (5.5 M in decane, 2.75 mmol) and complex **1** (18 µmol) or HM-Mo (17.3 mg, 8.1 µmol Mo): the amount of HM-Mo was chosen to have a reasonable catalyst bulk density and that of complex **1** to facilitate comparison with previously reported oxomolybdenum(VI) complexes used as epoxidation catalysts. The reactions were carried out without a cosolvent. The choice of the oxidant resides in the fact that it is known that [Mo(O)$_2$Cl$_2$]-type complexes are not very water stable because of the hydrolysis of the halide ligand in the presence of an excess amount of water.

The course of the reactions was monitored by using a Varian 3900 GC equipped with a capillary column (SPB-5, 20 m × 0.25 mm) and a flame-ionisation detector. For quantification of the products, nonane or undecane was used as an internal standard (withdrawn samples were added to diluted standard solutions): %(olefin conversion at time *t*) = [(initial concentration) – (concentration at time *t*)]/(initial concentration) × 100. The reaction products were identified by GC–MS [Trace GC 2000 Series (Thermo Quest CE Instruments)/DSQ II (Thermo Scientific)] by using He as carrier gas.

Acknowledgments

The authors are grateful to the Programa Operacional Ciência e Inovação/2010, the Fundo Europeu de Desenvolvimento Regional and the Fundação para a Ciência e a Tecnologia for financial support (POCI/CTM/ 55648/2004 and PPCDT/CTM/55648/2004).

[1] F. Hoffmann, M. Cornelius, J. Morell, M. Fröba, *Angew. Chem. Int. Ed.* **2006**, *45*, 3216–3251.
[2] J. H. Clark, D. J. Macquarrie, *Chem. Commun.* **1998**, 853–860.
[3] M. Dusi, T. Mallat, A. Baiker, *Catal. Rev. Sci. Eng.* **2000**, *42*, 213–278.

[4] I. W. C. E. Arends, R. A. Sheldon, *Appl. Catal. A* **2001**, *212*, 175–187.
[5] D. E. De Vos, M. Dams, B. F. Sels, P. A. Jacobs, *Adv. Synth. Catal.* **2003**, *345*, 457–473.
[6] J.-M. Brégeault, *Dalton Trans.* **2003**, 3289–3302.
[7] a) M. Schulz, J. H. Teles, J. Sundermeyer, G. Wahl, (BASF AG) DE Patent 195.33.31.4, **1995**; b) M. Schulz, J. H. Teles, J. Sundermeyer, G. Wahl, (BASF AG) WO Patent 10054, **1995**.
[8] a) H. Mimoun, I. Seree de Roch, L. Sajus, *Bull. Soc. Chim. Fr.* **1969**, 1481–1492; b) H. Mimoun, I. Seree de Roch, L. Sajus, *Tetrahedron* **1970**, *26*, 37–50.
[9] K. Jeyakumar, D. K. Chand, *J. Chem. Sci.* **2009**, *121*,111–123.
[10] C. Freund, W. Herrmann, F. E. Kühn, *Top. Organomet. Chem.* **2007**, *22*, 39–77.
[11] S. M. Bruno, C. C. L. Pereira, M. S. Balula, M. Nolasco, A. A. Valente, A. Hazell, M. Pillinger, P. R. Claro, I. S. Gonçalves, *J. Mol. Catal. A* **2007**, *261*, 79–87.
[12] S. M. Bruno, M. S. Balula, A. A. Valente, F. A. A. Paz, M. Pillinger, C. Sousa, J. Klinowski, C. Freire, P. R. Claro, I. S. Gonçalves, *J. Mol. Catal. A* **2007**, *270*, 185–194.
[13] Ž. Petrovski, M. Pillinger, A. A. Valente, I. S. Gonçalves, A. Hazell, C. C. Romão, *J. Mol. Catal. A* **2005**, *227*, 67–73.
[14] F. E. Kühn, A. M. Santos, A. D. Lopes, I. S. Gonçalves, J. E. R. Borges, M. Pillinger, C. C. Romão, *J. Organomet. Chem.* **2001**, *621*, 207–217.
[15] S. Gago, J. E. R. Borges, C. Teixeira, A. M. Santos, J. Zhao, M. Pillinger, C. D. Nunes, Ž. Petrovski, T. M. Santos, F. E. Kühn, C. C. Romão, I. S. Gonçalves, *J. Mol. Catal. A* **2005**, *236*, 1–6.
[16] F. E. Kühn, E. Herdtweck, J. J. Haider, W. A. Herrmann, I. S. Gonçalves, A. D. Lopes, C. C. Romão, *J. Organomet. Chem.* **1999**, *583*, 3–10.
[17] F. E. Kühn, A. D. Lopes, A. M. Santos, E. Herdtweck, J. J. Haider, C. C. Romão, A. G. Santos, *J. Mol. Catal. A* **2000**, *151*, 147–160.
[18] F. E. Kühn, A. M. Santos, A. D. Lopes, I. S. Gonçalves, E. Herdtweck, C. C. Romão, *J. Mol. Catal. A* **2000**, *164*, 25–38.
[19] K. R. Jain, F. E. Kühn, *Dalton Trans.* **2008**, 2221–2227.
[20] C. D. Nunes, A. A. Valente, M. Pillinger, A. C. Fernandes, C. C. Romão, J. Rocha, I. S. Gonçalves, *J. Mater. Chem.* **2002**, *12*, 1735–1742.
[21] C. D. Nunes, M. Pillinger, A. A. Valente, J. Rocha, A. D. Lopes, I. S. Gonçalves, *Eur. J. Inorg. Chem.* **2003**, 3870–3877.
[22] P. Ferreira, I. S. Gonçalves, F. E. Kühn, A. D. Lopes, M. A. Martins, M. Pillinger, A. Pina, J. Rocha, C. C. Romão, A. M. Santos, T. M. Santos, A. A. Valente, *Eur. J. Inorg. Chem.* **2000**, 2263–2270.
[23] M. Jia, W. R. Thiel, *Chem. Commun.* **2002**, 2392–2393.
[24] M. Jia, A. Seifert, W. R. Thiel, *Chem. Mater.* **2003**, *15*, 2174–2180.
[25] S. Tangestaninejad, M. H. Habibi, V. Mirkhani, M. Moghadam, G. Grivani, *Inorg. Chem. Commun.* **2006**, *9*, 575–578.
[26] M. Jia, A. Steifert, M. Berger, H. Giegengack, S. Schulze, W. R. Thiel, *Chem. Mater.* **2004**, *16*, 877–882.
[27] M. Jia, A. Steifert, W. R. Thiel, *J. Catal.* **2004**, *221*, 319–324.
[28] A. Castro, J. C. Alonso, P. Neves, A. A. Valente, P. Ferreira, *Eur. J. Inorg. Chem.* **2010**, 602–607.
[29] F. R. Fronczek, R. L. Luck, G. Wang, *Inorg. Chim. Acta* **2003**, *342*, 247–254.
[30] a) S. Inagaki, S. Guan, T. Ohsuna, O. Terasaki, *Nature* **2002**, *416*, 304–307; b) N. Bion, P. Ferreira, A. A. Valente, I. S. Gonçalves, J. Rocha, *J. Mater. Chem.* **2003**, *13*, 1910–1913.
[31] a) Y. Goto, S. Inagaki, *Chem. Commun.* **2002**, 2410–2411; b) Y. Goto, K. Okamoto, S. Inagaki, *Bull. Chem. Soc. Jpn.* **2005**, *78*, 932–936.
[32] S. J. Gregg, K. S. W. Sing, *Adsorption, Surface Area and Porosity*, 2nd ed., Academic Press, London, **1982**, ch. 2, p. 150.
[33] J. Blümel, *Inorg. Chem.* **1994**, *33*, 5050–5056.
[34] A. Jimtaisong, R. Luck, *Inorg. Chem.* **2006**, *45*, 10391–10402.
[35] R. Clarke, D. J. Cole-Hamilton, *J. Chem. Soc., Dalton Trans.* **1993**, 1913–1914.
[36] W. A. Herrmann, J. J. Haider, J. Fridgen, G. M. Lobmaier, M. Spiegler, *J. Organomet. Chem.* **2000**, *603*, 69–79.
[37] F. E. Kühn, A. M. Santos, A. D. Lopes, I. S. Gonçalves, J. E. Rodríguez-Borges, M. Pillinger, C. C. Romão, *J. Organomet. Chem.* **2001**, *621*, 207–217.
[38] S. M. Bruno, B. Monteiro, M. S. Balula, F. M. Pedro, M. Abrantes, A. A. Valente, M. Pillinger, P. Ribeiro-Claro, F. E. Kühn, I. S. Gonçalves, *J. Mol. Catal. A* **2006**, *260*, 11–18.
[39] I. S. Gonçalves, A. M. Santos, C. C. Romão, A. D. Lopes, J. E. Rodríguez-Borges, M. Pillinger, P. Ferreira, J. Rocha, F. E. Kühn, *J. Organomet. Chem.* **2001**, *626*, 1–10.
[40] S. Gago, J. E. Rodríguez-Borges, C. Teixeira, A. M. Santos, J. Zhao, M. Pillinger, C. D. Nunes, Ž. Petrovski, T. M. Santos, F. E. Kühn, C. C. Romão, I. S. Gonçalves, *J. Mol. Catal. A* **2005**, *236*, 1–6.
[41] J. Zhao, X. Zhou, A. M. Santos, E. Herdtweck, C. C. Romão, F. E. Kühn, *Dalton Trans.* **2003**, 3736–3742.
[42] J. A. Brito, M. Gómez, G. Muller, H. Teruel, J.-C. Clinet, E. Duñach, M. A. Maestro, *Eur. J. Inorg. Chem.* **2004**, 4278–4285.
[43] A. Al-Ajlouni, A. A. Valente, C. D. Nunes, M. Pillinger, A. M. Santos, J. Zhao, C. C. Romão, I. S. Gonçalves, F. E. Kühn, *Eur. J. Inorg. Chem.* **2005**, 1716–1723.
[44] F. E. Kühn, M. Groarke, É. Bencze, E. Herdtweck, A. Prazeres, A. M. Santos, M. J. Calhorda, C. C. Romão, I. S. Gonçalves, A. D. Lopes, M. Pillinger, *Chem. Eur. J.* **2002**, *8*, 2370–2383.
[45] L. F. Veiros, A. Prazeres, P. J. Costa, C. C. Romão, F. E. Kühn, M. J. Calhorda, *Dalton Trans.* **2006**, 1383–1389.
[46] D. V. Deubel, J. Sundermeyer, G. Frenking, *Eur. J. Inorg. Chem.* **2001**, 1819–1827 and references cited therein.
[47] A. Hroch, G. Gemmecker, W. R. Thiel, *Eur. J. Inorg. Chem.* **2000**, 1107–1114.
[48] S. Shylesh, M. Jia, A. Seifert, S. Adappa, S. Ernsta, W. R. Thiel, *New J. Chem.* **2009**, *33*, 717–719.
[49] G. M. Sheldrick, *Acta Crystallogr., Sect. A* **1990**, *46*, 467–473.
[50] G. M. Sheldrick, *SHELXL-97, Computer Program for Crystal Structure Refinement*, University of Göttingen, Göttingen, Germany, **1997**.
[51] A. L. Spek, *PLATON, A Multipurpose Crystallographic Tool*, Utrecht University, Utrecht, Netherlands, **2008**.
[52] M. B. Hursthouse, W. Levason, R. Ratnani, G. Reid, *Polyhedron* **2004**, *23*, 1915–1921.
[53] a) R. J. Angelici, H. Gao, *US Pat.* 5 789 333, **1998**; b) M. Capka, *Synth. React. Inorg. Met.-Org. Chem.* **1977**, *7*, 347–354.
[54] J. P. Bezombes, C. Chuit, R. J. P. Corriu, C. Reyé, *J. Mater. Chem.* **1999**, *9*, 1727–1734.

Received: November 10, 2009